A&A 585, A126 (2016)
DOI: 10.1051/0004-6361/201527276


Astronomy & Astrophysics

# Three irradiated and bloated hot Jupiters:

## WASP-76b, WASP-82b, and WASP-90b⋆

R. G. West[1], C. Hellier[2], J.-M. Almenara[3], D. R. Anderson[2], S. C. C. Barros[3], F. Bouchy[4,5], D. J. A. Brown[1], A. Collier Cameron[6], M. Deleuil[3], L. Delrez[7], A. P. Doyle[1,2], F. Faedi[1], A. Fumel[7], M. Gillon[7], Y. Gómez Maqueo Chew[1], G. Hébrard[4], E. Jehin[7], M. Lendl[7,8], P. F. L. Maxted[2], F. Pepe[8], D. Pollacco[1], D. Queloz[8,9], D. Ségransan[8], B. Smalley[2], A. M. S. Smith[2,10], J. Southworth[2], A. H. M. J. Triaud[8,11,12], and S. Udry[8]

[1] Department of Physics, University of Warwick, Coventry CV4 7AL, UK
e-mail: richard.west@warwick.ac.uk
[2] Astrophysics Group, Keele University, Staffordshire, ST5 5BG, UK
[3] Aix-Marseille Université, CNRS, LAM (Laboratoire d'Astrophysique de Marseille) UMR 7326, 13388 Marseille, France
[4] Institut d'Astrophysique de Paris, UMR 7095 CNRS, Université Pierre & Marie Curie, 75000 Paris, France
[5] Observatoire de Haute-Provence, CNRS/OAMP, 04870 St. Michel l'Observatoire, France
[6] SUPA, School of Physics and Astronomy, University of St. Andrews, North Haugh, Fife, KY16 9SS, UK
[7] Institut d'Astrophysique et de Géophysique, Université de Liège, Allée du 6 Août 17, Bât. B5C, Liège 1, Belgium
[8] Observatoire astronomique de l'Université de Genève, 51 Ch. des Maillettes, 1290 Sauverny, Switzerland
[9] Cavendish Laboratory, J J Thomson Avenue, Cambridge, CB3 0HE, UK
[10] N. Copernicus Astronomical Centre, Polish Academy of Sciences, Bartycka 18, 00-716 Warsaw, Poland
[11] Centre for Planetary Sciences, University of Toronto at Scarborough, 1265 Military Trail, Toronto, ON M1C 1A4, Canada
[12] Department of Astronomy & Astrophysics, University of Toronto, Toronto, ON M5S 3H4, Canada

Received 31 August 2015 / Accepted 8 October 2015

**ABSTRACT**

We report on three new transiting hot Jupiter planets, discovered from the WASP surveys, which we combine with radial velocities from OHP/SOPHIE and *Euler*/CORALIE and photometry from *Euler* and TRAPPIST. The planets WASP-76b, WASP-82b, and WASP-90b are all inflated, with radii of 1.7–1.8 $R_{\rm Jup}$. All three orbit hot stars, of type F5–F7, with orbits of 1.8–3.9 d, and all three stars have evolved, post-main-sequence radii (1.7–2.2 $R_\odot$). Thus the three planets fit a known trend of hot Jupiters that receive high levels of irradiation being highly inflated. We caution, though, about the presence of a selection effect, in that non-inflated planets around ~2 $R_\odot$ post-MS stars can often produce transits too shallow to be detected by the ground-based surveys that have found the majority of transiting hot Jupiters.

**Key words.** planetary systems – stars: individual: WASP-76 – stars: individual: WASP-82 – stars: individual: WASP-90

## 1. Introduction

The naive expectation that a Jupiter-mass planet would have a radius of one Jupiter has been replaced by the realisation that many of the hot Jupiters found by transit surveys have inflated radii. Planets as large as ~2 $R_{\rm Jup}$ have been found (e.g. WASP-17b, Anderson et al. 2010; HAT-P-32b, Hartman et al. 2011).

It is also apparent that inflated planets are more likely to be found around hot stars. For example, Hartman et al. (2012) reported three new HAT-discovered planets, with radii of 1.6–1.7 $R_{\rm Jup}$, all transiting F-type stars. Similarly, Smalley et al. (2012) reported that WASP-78b and WASP-79b are 1.7-$R_{\rm Jup}$ planets that orbit F stars. Here we continue this theme by announcing three new hot Jupiters, again all inflated and all orbiting F stars.

For a discussion of the radii of transiting exoplanets see the paper by Weiss et al. (2013). It is likely that stellar irradiation plays an important role in inflating hot Jupiters, since no inflated planets are known that receive less than $2 \times 10^8$ erg s$^{-1}$ cm$^{-2}$ (Miller & Fortney 2011; Demory & Seager 2011). There is also an extensive literature discussing other mechanisms for inflating hot Jupiters, such as tidal dissipation (e.g. Leconte et al. 2010, and references therein) and Ohmic dissipation (e.g. Batygin & Stevenson 2010).

## 2. Observations

The three transiting-planet systems reported here are near the equator, and so have been observed by both the SuperWASP-North camera array on La Palma and by WASP-South at Sutherland in South Africa. Our methods all follow those in previous WASP discovery papers closely. The WASP camera arrays are described in Pollacco et al. (2006), while our planet-hunting methods are described in Collier Cameron et al. (2007b) and Pollacco et al. (2008)

⋆ Tables of the photometry and radial velocity are only available at the CDS via anonymous ftp to cdsarc.u-strasbg.fr (130.79.128.5) or via http://cdsarc.u-strasbg.fr/viz-bin/qcat?J/A+A/585/A126

**Table 1.** Observations.

| Facility | Date | Notes |
|---|---|---|
| **WASP-76:** | | |
| SuperWASP-North | 2008 Sep.–2010 Dec. | 12 800 points |
| WASP-South | 2008 Jul.–2009 Dec. | 7700 points |
| OHP/SOPHIE | 2011 Sep.–2011 Dec. | 9 RVs |
| *Euler*/CORALIE | 2012 Feb.–2012 Dec. | 8 RVs |
| TRAPPIST | 2011 Nov. 06 | *I* filter |
| TRAPPIST | 2012 Aug. 25 | *I* filter |
| EulerCAM | 2012 Oct. 13 | Gunn *r* filter |
| TRAPPIST | 2012 Oct. 31 | *I* filter |
| TRAPPIST | 2012 Nov. 20 | *I* filter |
| **WASP-82:** | | |
| SuperWASP-North | 2008 Oct.–2011 Feb. | 15 100 points |
| WASP-South | 2008 Oct.–2010 Jan. | 8600 points |
| OHP/SOPHIE | 2011 Dec.–2012 Feb. | 8 RVs |
| *Euler*/CORALIE | 2012 Feb.–2013 Mar. | 20 RVs |
| EulerCAM | 2012 Nov. 20 | Gunn *r* filter |
| **WASP-90:** | | |
| SuperWASP-North | 2004 May–2010 Oct. | 40 800 points |
| WASP-South | 2008 Jun.–2009 Oct. | 12 200 points |
| *Euler*/CORALIE | 2011 Oct.–2012 Sep. | 15 RVs |
| TRAPPIST | 2012 Jun. 03 | $I+z$ filter |
| EulerCAM | 2012 Jul. 28 | Gunn *r* filter |
| TRAPPIST | 2012 Sep. 13 | $I+z$ filter |
| EulerCAM | 2013 Jun. 10 | Gunn *r* filter |

Equatorial WASP candidates are followed up by obtaining radial velocities using the SOPHIE spectrograph on the 1.93-m telescope at Observatoire de Haute-Provence (as described in, e.g. Hébrard et al. 2013) and the CORALIE spectrograph on the 1.2-m *Euler* telescope at La Silla (e.g. Triaud et al. 2013). Higher-quality light curves of transits are obtained using EulerCAM on the 1.2-m telescope (e.g. Lendl et al. 2012) and the robotic TRAPPIST photometer at La Silla (e.g. Gillon et al. 2013). The observations for our three new planets are listed in Table 1.

## 3. The host stars

The stellar parameters for WASP-76, WASP-82, and WASP-90 were derived by co-adding the spectra from the radial-velocity measurements and analysing the summed spectrum using the methods given in Doyle et al. (2013). The excitation balance of the Fe I lines was used to determine the effective temperature ($T_{\rm eff}$). The surface gravity ($\log g$) was determined from the ionisation balance of Fe I and Fe II. The Ca I line at 6439 Å and the Na I D lines were also used as $\log g$ diagnostics. Values of microturbulence ($\xi_{\rm t}$) were obtained by requiring a null-dependence on abundance with equivalent width. The elemental abundances were determined from equivalent width measurements of several unblended lines. The quoted error estimates include those given by the uncertainties in $T_{\rm eff}$ and $\log g$, as well as the scatter due to measurement and atomic data uncertainties. The projected stellar rotation velocity ($v \sin I$) was determined by fitting the profiles of several unblended Fe I lines. Macroturbulence was obtained from the calibration by Bruntt et al. (2010).

For WASP-76, the rotation rate ($P = 17.6 \pm 4.0$ d) implied by the $v \sin I$ (assuming that the spin axis is perpendicular to us) gives a gyrochronological age of $5.3^{+6.1}_{-2.9}$ Gyr, using the Barnes (2007) relation. The lithium age of several Gyr, estimated using results in Sestito & Randich (2005), is consistent. For WASP-90, the rotation rate ($P = 11.1 \pm 1.6$ d), implied by the $v \sin I$, gives a gyrochronological age of $4.4^{+8.4}_{-2.4}$ Gyr. The $T_{\rm eff}$ of this star is close to the lithium-gap (Böhm-Vitense 2004), and thus the lack of any detectable lithium in this star does not provide a usable age constraint. WASP-82 is too hot for reliable gyrochronological or lithium ages.

In Tables 2–4 we list the proper motions of the three stars from the UCAC4 catalogue (Zacharias et al. 2013). These are compatible with the stars from the local thin-disc population. We also searched the WASP photometry of each star for rotational modulations by using a sine-wave fitting algorithm as described by Maxted et al. (2011). No significant periodicity (<1 mmag at 95%-confidence) was found for any of the three stars.

**Table 2.** System parameters for WASP-76.

| | |
|---|---|
| BD+01 316 | |
| 1SWASP J014631.86+024202.0 | |
| 2MASS 01463185+0242019 | |
| RA = $01^{\rm h}46^{\rm m}31.86^{\rm s}$, Dec = +02°42′02.0″ (J2000) | |
| $V$ mag = 9.5 | |
| Rotational modulation | <1 mmag (95%) |
| pm (RA) 46.6 ± 0.7 (Dec), –39.9 ± 0.6 mas/yr | |
| Stellar parameters from spectroscopic analysis | |
| Spectral type | F7 |
| $T_{\rm eff}$ (K) | 6250 ± 100 |
| $\log g$ | 4.4 ± 0.1 |
| $\xi_{\rm t}$ (km s$^{-1}$) | 1.4 ± 0.1 |
| $v_{\rm mac}$ (km s$^{-1}$) | 4.0 ± 0.3 |
| $v \sin I$ (km s$^{-1}$) | 3.3 ± 0.6 |
| [Fe/H] | +0.23 ± 0.10 |
| log A(Li) | 2.28 ± 0.10 |
| Distance (pc) | 120 ± 20 |
| Parameters from MCMC analysis | |
| $P$ (d) | 1.809886 ± 0.000001 |
| $T_{\rm c}$ (HJD) (UTC) | 245 6107.85507 ± 0.00034 |
| $T_{14}$ (d) | 0.1539 ± 0.0008 |
| $T_{12} = T_{34}$ (d) | $0.0154^{+0.0008}_{-0.0003}$ |
| $\Delta F = R_{\rm P}^2/R_*^2$ | 0.01189 ± 0.00016 |
| $b$ | $0.14^{+0.11}_{-0.09}$ |
| $i$ (°) | $88.0^{+1.3}_{-1.6}$ |
| $K_1$ (km s$^{-1}$) | 0.1193 ± 0.0018 |
| $\gamma$ (km s$^{-1}$) | –1.0733 ± 0.0002 |
| $e$ | 0 (adopted) (<0.05 at 3$\sigma$) |
| $M_*$ ($M_\odot$) | 1.46 ± 0.07 |
| $R_*$ ($R_\odot$) | 1.73 ± 0.04 |
| $\log g_*$ (cgs) | 4.128 ± 0.015 |
| $\rho_*$ ($\rho_\odot$) | $0.286^{+0.008}_{-0.018}$ |
| $T_{\rm eff}$ (K) | 6250 ± 100 |
| $M_{\rm P}$ ($M_{\rm Jup}$) | 0.92 ± 0.03 |
| $R_{\rm P}$ ($R_{\rm Jup}$) | $1.83^{+0.06}_{-0.04}$ |
| $\log g_{\rm P}$ (cgs) | 2.80 ± 0.02 |
| $\rho_{\rm P}$ ($\rho_{\rm J}$) | 0.151 ± 0.010 |
| $a$ (AU) | 0.0330 ± 0.0005 |
| $T_{\rm P,A\,=\,0}$ (K) | 2160 ± 40 |
| Errors are 1$\sigma$; Limb-darkening coefficients were: | |
| TRAPPIST $z$: | |
| a1 = 0.683, a2 = –0.349, a3 = 0.565, a4 = –0.286 | |
| EulerCAM $r_G$: | |
| a1 = 0.593, a2 = 0.021, a3 = 0.327, a4 = –0.215 | |

## 4. System parameters

The radial-velocity and photometric data (Table 1) were combined in a simultaneous Markov-chain Monte-Carlo (MCMC) analysis to find the system parameters (see

**Table 3.** System parameters for WASP-82.

| | |
|---|---|
| 1SWASP J045038.56+015338.1 | |
| 2MASS 04503856+0153381 | |
| RA = $04^h50^m38.56^s$, Dec = +01°53′38.1″ (J2000) | |
| $V$ mag = 10.1 | |
| Rotational modulation | <0.6 mmag (95%) |
| pm (RA) −17.5 ± 0.9 (Dec), −17.7 ± 0.7 mas/yr | |
| Stellar parameters from spectroscopic analysis | |
| Spectral type | F5 |
| $T_{\rm eff}$ (K) | 6500 ± 80 |
| log $g$ | 4.18 ± 0.09 |
| $\xi_{\rm t}$ (km s$^{-1}$) | 1.5 ± 0.1 |
| $v_{\rm mac}$(km s$^{-1}$) | 5.0 ± 0.3 |
| $v$ sin $I$ (km s$^{-1}$) | 2.6 ± 0.9 |
| [Fe/H] | +0.12 ± 0.11 |
| log A(Li) | 3.11 ± 0.08 |
| Distance (pc) | 200 ± 30 |
| Parameters from MCMC analysis | |
| $P$ (d) | 2.705782 ± 0.000003 |
| $T_{\rm c}$ (HJD) (UTC) | 245 6157.9898 ± 0.0005 |
| $T_{14}$ (d) | 0.2077 ± 0.0012 |
| $T_{12} = T_{34}$ (d) | $0.0156^{+0.0012}_{-0.0004}$ |
| $\Delta F = R_{\rm P}^2/R_*^2$ | 0.00624 ± 0.00012 |
| $b$ | $0.16^{+0.14}_{-0.11}$ |
| $i$ (°) | $87.9^{+1.4}_{-1.9}$ |
| $K_1$ (km s$^{-1}$) | 0.1307 ± 0.0019 |
| $\gamma$ (km s$^{-1}$) | –23.62827 ± 0.00007 |
| $e$ | 0 (adopted) (<0.06 at 3$\sigma$) |
| $M_*$ ($M_\odot$) | 1.63 ± 0.08 |
| $R_*$ ($R_\odot$) | $2.18^{+0.08}_{-0.05}$ |
| log $g_*$ (cgs) | $3.973^{+0.013}_{-0.02}$ |
| $\rho_*$ ($\rho_\odot$) | $0.158^{+0.006}_{-0.014}$ |
| $T_{\rm eff}$ (K) | 6490 ± 100 |
| $M_{\rm P}$ ($M_{\rm Jup}$) | 1.24 ± 0.04 |
| $R_{\rm P}$ ($R_{\rm Jup}$) | $1.67^{+0.07}_{-0.05}$ |
| log $g_{\rm P}$ (cgs) | $3.007^{+0.017}_{-0.032}$ |
| $\rho_{\rm P}$ ($\rho_{\rm J}$) | $0.266^{+0.017}_{-0.029}$ |
| $a$ (AU) | 0.0447 ± 0.0007 |
| $T_{\rm P,A=0}$ (K) | 2190 ± 40 |
| Errors are 1$\sigma$; Limb-darkening coefficients were: | |
| EulerCAM $r_G$: | |
| a1 = 0.494, a2 = 0.424, a3 = –0.266, a4 = 0.0436 | |

**Table 4.** System parameters for WASP-90.

| | |
|---|---|
| 1SWASP J210207.70+070323.7 | |
| 2MASS 21020767+0703224 | |
| RA = $21^h02^m07.70^s$, Dec = +07°03′23.7″ (J2000) | |
| $V$ mag = 11.7 | |
| Rotational modulation | <1 mmag (95%) |
| pm (RA) −10.2 ± 1.4 (Dec), 8.1 ± 4.3 mas/yr | |
| Stellar parameters from spectroscopic analysis | |
| Spectral type | F6 |
| $T_{\rm eff}$ (K) | 6440 ± 130 |
| log $g$ | 4.32 ± 0.09 |
| $\xi_{\rm t}$ (km s$^{-1}$) | 1.3 ± 0.2 |
| $v_{\rm mac}$(km s$^{-1}$) | 4.7 ± 0.3 |
| $v$ sin $I$ (km s$^{-1}$) | 6.0 ± 0.5 |
| [Fe/H] | +0.11 ± 0.14 |
| log A(Li) | <1.7 |
| Distance (pc) | 340 ± 60 |
| Parameters from MCMC analysis | |
| $P$ (d) | 3.916243 ± 0.000003 |
| $T_{\rm c}$ (HJD) (UTC) | 245 6235.5639 ± 0.0005 |
| $T_{14}$ (d) | 0.1398 ± 0.0022 |
| $T_{12} = T_{34}$ (d) | 0.033 ± 0.003 |
| $\Delta F = R_{\rm P}^2/R_*^2$ | 0.0071 ± 0.0002 |
| $b$ | 0.841 ± 0.013 |
| $i$ (°) | 82.1 ± 0.4 |
| $K_1$ (km s$^{-1}$) | 0.060 ± 0.006 |
| $\gamma$ (km s$^{-1}$) | 4.361 ± 0.0003 |
| $e$ | 0 (adopted) (<0.5 at 3$\sigma$) |
| $M_*$ ($M_\odot$) | 1.55 ± 0.10 |
| $R_*$ ($R_\odot$) | 1.98 ± 0.09 |
| log $g_*$ (cgs) | 4.033 ± 0.029 |
| $\rho_*$ ($\rho_\odot$) | 0.20 ± 0.02 |
| $T_{\rm eff}$ (K) | 6430 ± 130 |
| $M_{\rm P}$ ($M_{\rm Jup}$) | 0.63 ± 0.07 |
| $R_{\rm P}$ ($R_{\rm Jup}$) | 1.63 ± 0.09 |
| log $g_{\rm P}$ (cgs) | 2.73 ± 0.06 |
| $\rho_{\rm P}$ ($\rho_{\rm J}$) | 0.145 ± 0.027 |
| $a$ (AU) | 0.0562 ± 0.0012 |
| $T_{\rm P,A=0}$ (K) | 1840 ± 50 |
| Errors are 1$\sigma$; Limb-darkening coefficients were: | |
| TRAPPIST $I + z$: | |
| a1 = 0.554, a2 = 0.041, a3 = 0.070, a4 = –0.086 | |
| EulerCAM $r_G$: | |
| a1 = 0.476, a2 = 0.422, a3 = –0.226, a4 = 0.020 | |

Collier Cameron et al. 2007a for an account of our methods). For limb-darkening we used the four-parameter law from Claret (2000) and list the resulting parameters in Tables 2–4.

For WASP-76b and WASP-82b, the radial-velocity data imply circular orbits with eccentricities of less than 0.05 and 0.06 respectively (at 3$\sigma$). The star WASP-90 is fainter and WASP-90b is a lower-mass planet, so, while the data are again compatible with a circular orbit, the 3$\sigma$ limit on the eccentricity is weaker at 0.5. For all three, we enforced a circular orbit in the MCMC analysis (see Anderson et al. 2012 for the rationale for this). One of the WASP-82 RVs was taken during transit, and this point was given zero weight in the analysis. To translate transit and radial-velocity information (which give stellar density) into the star's mass and radius we need one additional mass–radius constraint. Here we use the calibration presented by Southworth (2011).

The fitted parameters were thus $T_{\rm c}$, $P$, $\Delta F$, $T_{14}$, $b$, $K_1$, where $T_{\rm c}$ is the epoch of mid-transit, $P$ is the orbital period, $\Delta F$ is the fractional flux-deficit that would be observed during transit in the absence of limb-darkening, $T_{14}$ is the total transit duration (from first to fourth contact), $b$ is the impact parameter of the planet's path across the stellar disc, and $K_1$ is the stellar reflex velocity semi-amplitude. The resulting fits are reported in Tables 2 to 4.

## 5. Discussion

The three host stars, WASP-76, WASP-82, and WASP-90, are all F stars with temperatures of 6250–6500 K. Their metallicities ([Fe/H] = 0.1–0.2) and space velocities are compatible with the local thin-disk population. The stellar densities derived from the MCMC analysis, along with the temperatures from

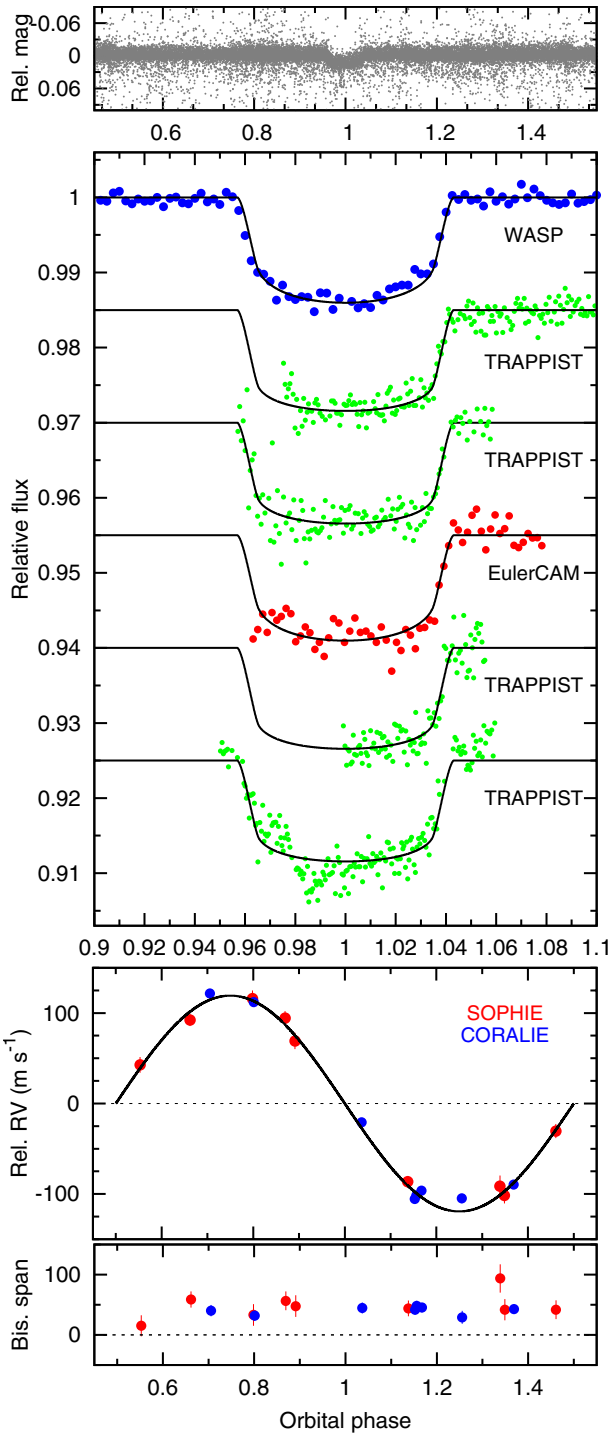


**Fig. 1.** WASP-76b discovery data: *top*: the WASP data folded on the transit period. *Second panel*: the binned WASP data with (offset) the follow-up transit light curves (ordered from the top as in Table 1) together with the fitted MCMC model. *Third*: The SOPHIE and CORALIE radial velocities with the fitted model. *Bottom*: The bisector spans; the absence of any correlation with radial velocity is a check against transit mimics.

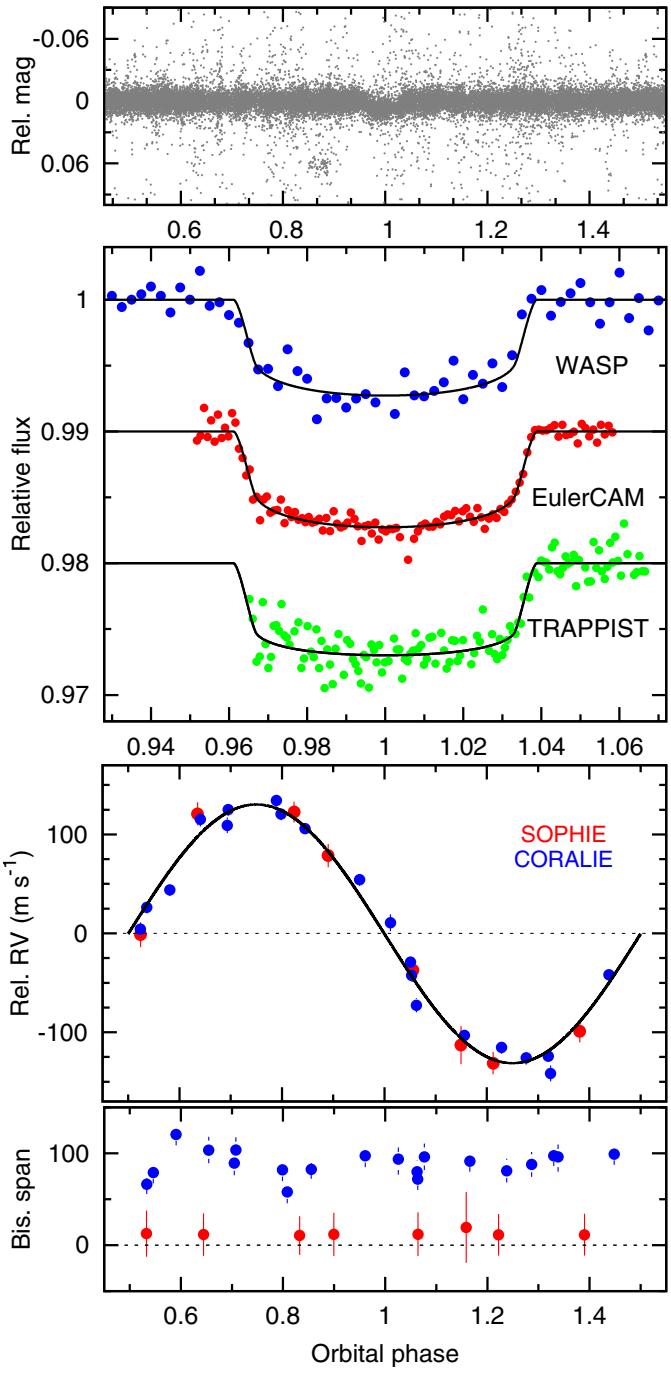


**Fig. 2.** WASP-82b discovery data (as for Fig. 1).

the spectral analysis, are shown on a modified Hertzsprung–Russell diagram in Fig. 4. All three stars have inflated radii ($R_* = 1.7$–$2.2\,R_\odot$), and thus appear to have evolved significantly. The indicated ages of ∼2 Gyr are compatible with the estimates from gyrochronology (see Sect. 2).

The stellar $\log g$ values from the spectroscopic analyses are generally higher than those from the transit analyses by 0.2–0.3, whereas the errors on the spectroscopic values are ≈0.1 (see Tables 2 to 4). The spectroscopic $T_{\rm eff}$ values, though, are consistent with the $T_{\rm eff}$ values from the Southworth (2011) calibration used in the MCMC analysis.

This $\log g$ discrepancy has occurred before in WASP analyses, particularly for F-type stars, and has been discussed by Smalley et al. (2012). For stars hotter than ≈6000 K there appears to be a systematic offset in spectroscopic $\log g$ of ≈0.2 (see their Fig. 6), and indeed the offset for the stars reported here is in line with that reported by Smalley et al. for WASP-78 and WASP-79. Bruntt et al. (2012) reported a similar discrepancy,

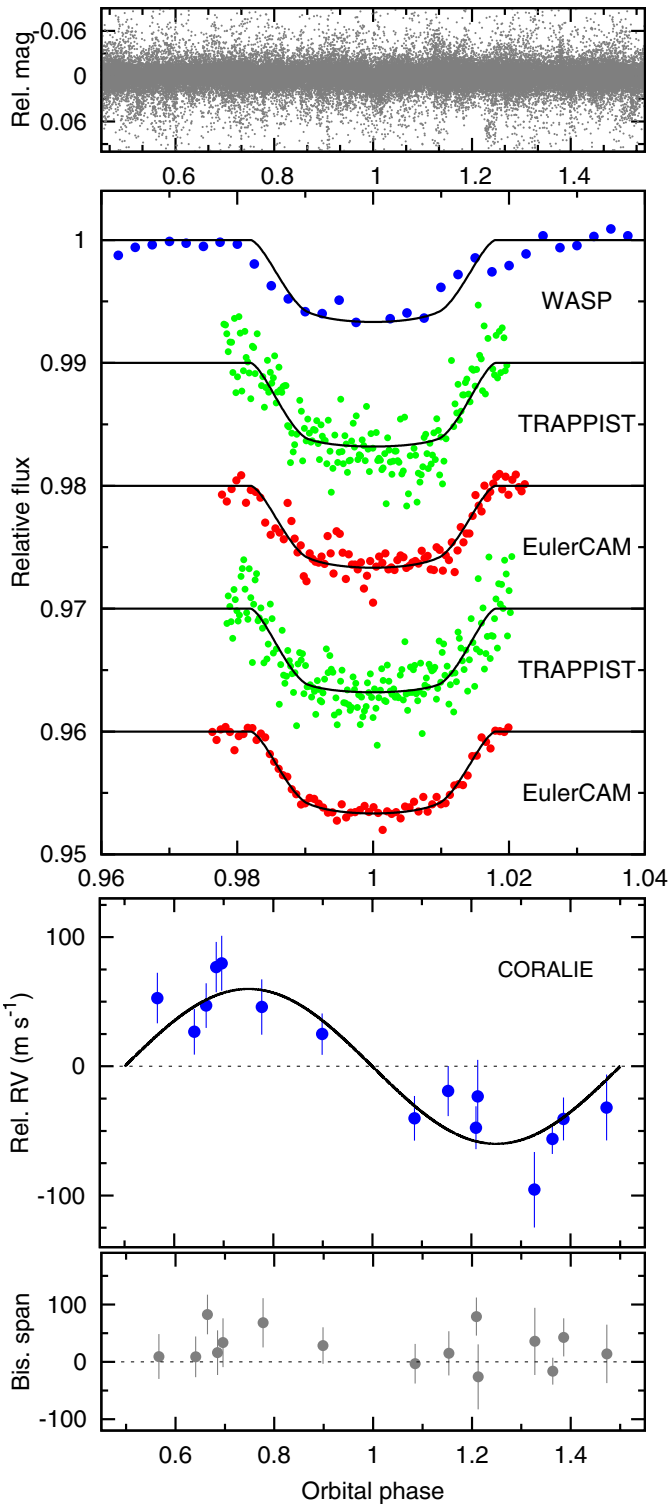


**Fig. 3.** WASP-90b discovery data (as for Fig. 1).

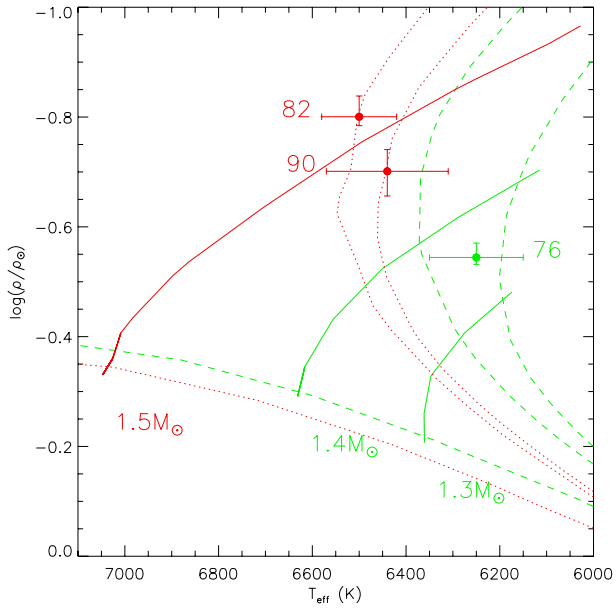


**Fig. 4.** Evolutionary tracks on a modified H-R diagram ($\rho$ versus $T_{\rm eff}$). The green lines show a metallicity of [Fe/H] = +0.19; the dashed lines indicate isochrones for 0.07, 2.0, and 2.5 Gyr; the solid lines indicate mass tracks for 1.3 $M_{\odot}$ and 1.4 $M_{\odot}$. The red lines indicate a metallicity of [Fe/H] = +0.1, with the same isochrones, and the mass track for 1.5 $M_{\odot}$. The models are from Girardi et al. (2000).

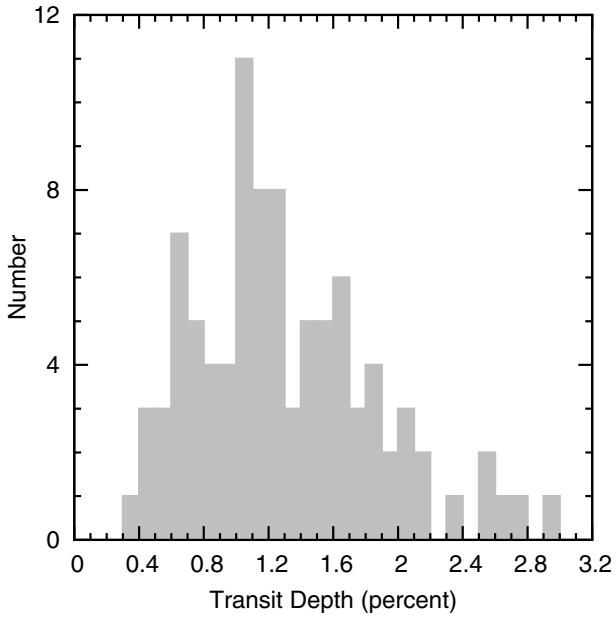


**Fig. 5.** Transit depths for all published WASP planet detections.

again for hotter stars, between spectroscopic $\log g$ values and $\log g$ values derived from asteroseismology. Smalley et al. (2012) suggest that the discepancy might be due to systematic non-LTE effects in the spectroscopic values for hotter stars.

While this offset is not fully understood, we regard the spectroscopic determination as the less reliable, compared to the more direct determination of stellar $\log g$ from the transit lightcurves. Thus, in line with previous WASP discovery papers, while we report the values from the spectroscopic analysis, the quoted stellar and planetary masses and radii (Tables 2 to 4) are derived using the $\log g$ from the transit analyses. We caution that the quoted errors for the MCMC analysis are those that are internal to the method, and do not include possible systematic biases.

At $V = 9.5$ and $R_{\rm P} = 1.8\ R_{\rm Jup}$, WASP-76 is now the brightest known star transited by a planet larger than 1.5 $R_{\rm Jup}$. WASP-82 is not far behind at $V = 10.1$ and $R_{\rm P} = 1.7\ R_{\rm Jup}$, comparable to WASP-79 ($V = 10.1$, $R_{\rm P} = 1.7\ R_{\rm Jup}$; Smalley et al. 2012) and KOI-13 ($V = 10.0$, $R_{\rm P} = 1.8\ R_{\rm Jup}$; Santerne et al. 2012). Thus the new discoveries will be useful for studying bloated hot Jupiters. For example, Triaud (2011) suggests that the orbital inclinations

of hot Jupiters are a function of system age. Given that radius changes of evolved systems give age constraints, WASP-76 and WASP-82 will be good systems for testing this idea. WASP-82 has a relatively small $v \sin I$ (Table 3) for its spectral type, which could indicate a misaligned orbit.

### 5.1. The radius–irradiation relation

Several papers have reported a relationship between the radii of known hot Jupiters and the irradiation they receive (e.g. Demory & Seager 2011; Weiss et al. 2013; Delrez et al. 2014). For planets with $M_P > 0.5\ M_{Jup}$, Weiss et al. (2013) fit $R_P \propto F^{0.09}$, where the irradiation $F \propto T_{eff}^4 R_*^2/a^2$.

The three planets reported here are highly irradiated, receiving 3–5 $\times 10^9$ erg cm$^{-2}$ s$^{-1}$ and have inflated radii of 1.6–1.8 $R_{Jup}$ (18–20 $R_{Earth}$). They fit the Weiss et al. relationship well (see their Fig. 14).

However, there is a strong selection effect operating. The high irradiation comes partly from the large stellar radii of 1.7–2.2 $R_\odot$, which means much shallower transits. Had these planets not had inflated radii, we probably would not have discovered them. The transit depths of the three planets are 1.2%, 0.6%, and 0.7% (for WASP-76, WASP-82b, and WASP-90b respectively). If they had had non-inflated radii of 1 $R_{Jup}$, then the transit depths would have been 0.36%, 0.22%, and 0.27%, respectively, at or below the WASP threshold (see Fig. 5).

There are only four WASP planets with transits depths shallower than 0.5%, with three at 0.4% (WASP-71b, WASP-72b, and WASP-99b; Gillon et al. 2013; Smith et al. 2013; Hellier et al. 2014) and the shallowest of all, WASP-73b at 0.33% (Delrez et al. 2014). This last is instructive as a non-inflated hot Jupiter (1.16 $R_{Jup}$) experiencing high irradiation ($2.3 \times 10^9$ erg cm$^{-2}$ s$^{-1}$) around a 2.1-$R_\odot$ F9 star. This discovery required the shallowest detection of all WASP transits.

Given that the majority of transiting hot Jupiters have been found by WASP and the similar ground-based survey HATnet (Bakos et al. 2002), the absence of highly-irradiated but normal-radius Jupiters could simply be a selection effect. The effect of this bias is not straightforward to evaluate since WASP transit searching on brighter stars is limited by red noise, rather than by photon statistics, and so the decrease in sensitivity as transits get shallower is not a simple function.

We note, though, that the irradiation–radius relation (e.g. Fig. 9 of Delrez et al. 2014) results not only from the absence of non-inflated planets around large, hot stars (which could be a selection effect) but also the absence of highly inflated planets (1.5–1.8 $R_{Jup}$) around cooler, smaller stars. Such planets would produce deep transits and so would be obvious in transit surveys. WASP-South has routinely pursued candidates with projected radii up to 2.2 $R_{Jup}$, and has no known selection effects against planets in the 1.5–1.8 $R_{Jup}$ range transiting G and K stars.

Delrez et al. (2014) suggest that one of the reasons for the bloated size of WASP-88b (1.7 $R_{Jup}$) might be its relatively low mass (0.56 $M_{Jup}$) and relatively low metallicity ([Fe/H] = –0.08). The three bloated planets reported have higher masses (0.6, 0.9, and 1.2 $M_{Jup}$) and higher metallicities (+0.1 to +0.2) which implies that highly inflated planets are seen at a range of masses and metallicities.

Thus, despite the concerns about selection effects discussed here, the correlation with irradiation may still be the best explanation for the inflated radii of some hot Jupiters (see, e.g. Showman & Guillot 2002), though other mechanisms such as tidal dissipation (e.g. Leconte et al. 2010) may also be important.

*Acknowledgements.* SuperWASP-North is hosted by the Issac Newton Group and the Instituto de Astrofísica de Canarias on La Palma while WASP-South is hosted by the South African Astronomical Observatory; we are grateful for their ongoing support and assistance. Funding for WASP comes from consortium universities and from the UK's Science and Technology Facilities Council. TRAPPIST is funded by the Belgian Fund for Scientific Research (Fond National de la Recherche Scientifique, FNRS), under the grant FRFC 2.5.594.09.F, with the participation of the Swiss National Science Fundation (SNF). M. Gillon and E. Jehin are FNRS Research Associates.

## References

Anderson, D. R., Hellier, C., Gillon, M., et al. 2010, ApJ, 709, 159
Anderson, D. R., Collier Cameron, A., Gillon, M., et al. 2012, MNRAS, 422, 1988
Bakos, G. Á., Lázár, J., Papp, I., Sári, P., & Green, E. M. 2002, PASP, 114, 974
Barnes, S. A. 2007, ApJ, 669, 1167
Batygin, K., & Stevenson, D. J. 2010, ApJ, 714, L238
Böhm-Vitense, E. 2004, AJ, 128, 2435
Bruntt, H., Bedding, T. R., Quirion, P.-O., et al. 2010, MNRAS, 405, 1907
Bruntt, H., Basu, S., Smalley, B., et al. 2012, MNRAS, 423, 122
Claret, A. 2000, A&A, 363, 1081
Collier Cameron, A., Bouchy, F., Hébrard, G., et al. 2007a, MNRAS, 375, 951
Collier Cameron, A., Wilson, D. M., West, R. G., et al. 2007b, MNRAS, 380, 1230
Delrez, L., Van Grootel, V., Anderson, D. R., et al. 2014, A&A, 563, A143
Demory, B.-O., & Seager, S. 2011, ApJS, 197, 12
Doyle, A. P., Smalley, B., Maxted, P. F. L., et al. 2013, MNRAS, 428, 3164
Gillon, M., Anderson, D. R., Collier-Cameron, A., et al. 2013, A&A, 552, A82
Girardi, L., Bressan, A., Bertelli, G., & Chiosi, C. 2000, A&AS, 141, 371
Hartman, J. D., Bakos, G. Á., Torres, G., et al. 2011, ApJ, 742, 59
Hartman, J. D., Bakos, G. Á., Béky, B., et al. 2012, AJ, 144, 139
Hébrard, G., Collier Cameron, A., Brown, D. J. A., et al. 2013, A&A, 549, A134
Hellier, C., Anderson, D. R., Cameron, A. C., et al. 2014, MNRAS, 440, 1982
Leconte, J., Chabrier, G., Baraffe, I., & Levrard, B. 2010, A&A, 516, A64
Lendl, M., Anderson, D. R., Collier-Cameron, A., et al. 2012, A&A, 544, A72
Maxted, P. F. L., Anderson, D. R., Collier Cameron, A., et al. 2011, PASP, 123, 547
Miller, N., & Fortney, J. J. 2011, ApJ, 736, L29
Pollacco, D. L., Skillen, I., Collier Cameron, A., et al. 2006, PASP, 118, 1407
Pollacco, D., Skillen, I., Collier Cameron, A., et al. 2008, MNRAS, 385, 1576
Santerne, A., Moutou, C., Barros, S. C. C., et al. 2012, A&A, 544, L12
Sestito, P., & Randich, S. 2005, A&A, 442, 615
Showman, A. P., & Guillot, T. 2002, A&A, 385, 166
Smalley, B., Anderson, D. R., Collier-Cameron, A., et al. 2012, A&A, 547, A61
Smith, A. M. S., Anderson, D. R., Bouchy, F., et al. 2013, A&A, 552, A120
Southworth, J. 2011, MNRAS, 417, 2166
Triaud, A. H. M. J. 2011, A&A, 534, L6
Triaud, A. H. M. J., Anderson, D. R., Collier Cameron, A., et al. 2013, A&A, 551, A80
Weiss, L. M., Marcy, G. W., Rowe, J. F., et al. 2013, ApJ, 768, 14
Zacharias, N., Finch, C. T., Girard, T. M., et al. 2013, AJ, 145, 44

## Appendix A: Tables of the radial velocities

**Table A.1.** Radial velocities.

| BJD – 2 400 000 (UTC) | RV (km s$^{-1}$) | $\sigma_{RV}$ (km s$^{-1}$) | Bisector (km s$^{-1}$) |
|---|---|---|---|
| **WASP-76: CORALIE** | | | |
| 55 961.53656 | −1.1983 | 0.0042 | 0.0485 |
| 55 962.53148 | −0.9749 | 0.0047 | 0.0404 |
| 56 111.93690 | −1.2014 | 0.0054 | 0.0291 |
| 56 112.92459 | −0.9846 | 0.0043 | 0.0318 |
| 56 236.65993 | −1.1929 | 0.0041 | 0.0457 |
| 56 249.69408 | −1.1862 | 0.0037 | 0.0428 |
| 56 265.59101 | −1.2021 | 0.0041 | 0.0417 |
| 56 272.62129 | −1.1174 | 0.0045 | 0.0447 |
| **WASP-76: SOPHIE** | | | |
| 55 830.57771 | −0.9573 | 0.0090 | 0.0331 |
| 55 831.57367 | −1.1750 | 0.0088 | 0.0418 |
| 55 832.55517 | −1.0042 | 0.0090 | 0.0478 |
| 55 833.58663 | −1.1038 | 0.0078 | 0.0417 |
| 55 855.47129 | −1.0307 | 0.0087 | 0.0152 |
| 55 856.52991 | −1.1599 | 0.0066 | 0.0440 |
| 55 857.47859 | −0.9810 | 0.0067 | 0.0586 |
| 55 900.33148 | −1.1648 | 0.0118 | 0.0936 |
| 55 901.29156 | −0.9789 | 0.0078 | 0.0565 |
| **WASP-82: CORALIE** | | | |
| 55 974.61462 | −23.7388 | 0.0065 | 0.0811 |
| 55 976.57143 | −23.5694 | 0.0062 | 0.0972 |
| 55 979.55186 | −23.6661 | 0.0063 | 0.0798 |
| 55 981.54352 | −23.4891 | 0.0062 | 0.0820 |
| 55 982.53631 | −23.7268 | 0.0056 | 0.0913 |
| 55 983.53088 | −23.6192 | 0.0053 | 0.0664 |
| 55 992.51846 | −23.5177 | 0.0052 | 0.0825 |
| 55 994.50952 | −23.5795 | 0.0059 | 0.1206 |
| 55 996.50877 | −23.7477 | 0.0056 | 0.0974 |
| 55 997.52351 | −23.4983 | 0.0066 | 0.0894 |
| 55 999.53457 | −23.6654 | 0.0058 | 0.0991 |
| 56 000.50857 | −23.5030 | 0.0061 | 0.0578 |
| 56 002.50493 | −23.5973 | 0.0059 | 0.0790 |
| 56 004.50833 | −23.7495 | 0.0068 | 0.0880 |
| 56 225.77254 | −23.6525 | 0.0060 | 0.0720 |
| 56 354.53934 | −23.5082 | 0.0072 | 0.1035 |
| 56 355.54337 | −23.6129 | 0.0085 | 0.0937 |
| 56 364.50632 | −23.7652 | 0.0080 | 0.0962 |
| 56 365.50555 | −23.5143 | 0.0079 | 0.1038 |
| 56 366.50386 | −23.6962 | 0.0072 | 0.0961 |
| **WASP-82: SOPHIE** | | | |
| 55 924.30590 | −23.5070 | 0.0116 | 0.0377 |
| 55 925.44261 | −23.6651 | 0.0119 | 0.0122 |
| 55 926.32456 | −23.7267 | 0.0114 | 0.0451 |
| 55 929.41641 | −23.6291 | 0.0126 | 0.0787 |
| 55 930.40736 | −23.5492 | 0.0117 | 0.0650 |
| 55 936.52005 | −23.7408 | 0.0193 | 0.1027 |
| 55 938.34462 | −23.5051 | 0.0105 | 0.0801 |
| 55977.27640 | −23.7591 | 0.0113 | 0.1159 |

Bisector errors are twice RV errors

**Table A.2.** Radial velocities.

| BJD – 2 400 000 (UTC) | RV (km s$^{-1}$) | $\sigma_{RV}$ (km s$^{-1}$) | Bisector (km s$^{-1}$) |
|---|---|---|---|
| **WASP-90: CORALIE** | | | |
| 55 850.58112 | 4.4406 | 0.0213 | 0.0333 |
| 55 852.60464 | 4.3376 | 0.0283 | −0.026 |
| 55 888.52841 | 4.3201 | 0.0166 | 0.0427 |
| 55 889.52682 | 4.3876 | 0.0177 | 0.0086 |
| 55 890.53714 | 4.3857 | 0.0159 | 0.0282 |
| 55 891.53405 | 4.3417 | 0.0193 | 0.0148 |
| 55 893.53766 | 4.4078 | 0.0172 | 0.0825 |
| 56 075.81618 | 4.3134 | 0.0166 | 0.0788 |
| 56 076.84883 | 4.3289 | 0.0255 | 0.0137 |
| 56 103.83463 | 4.3047 | 0.0117 | −0.016 |
| 56 136.78376 | 4.4067 | 0.0215 | 0.0681 |
| 56 149.73856 | 4.3205 | 0.0173 | −0.003 |
| 56 150.68690 | 4.2653 | 0.0292 | 0.0356 |
| 56 151.62369 | 4.4136 | 0.0196 | 0.0092 |
| 56 175.58669 | 4.4376 | 0.0194 | 0.0159 |

Bisector errors are twice RV errors